Journal of South American Earth Sciences 45 (2013) 345–356

Contents lists available at SciVerse ScienceDirect

Journal of South American Earth Sciences

journal homepage: www.elsevier.com/locate/jsames

Recent glacier variations on active ice capped volcanoes in the Southern Volcanic Zone (37°–46°S), Chilean Andes

Andrés Rivera [a,b], Francisca Bown [a,*]

[a] Centro de Estudios Científicos (CECs), Valdivia, Chile
[b] Departamento de Geografía, Universidad de Chile, Santiago, Chile

ARTICLE INFO

Article history:
Received 12 October 2011
Accepted 27 February 2013

Keywords:
Ice-capped active volcanoes
Glacier recession
Glacier–volcano interactions

ABSTRACT

Glaciers in the southern province of the Southern Volcanic Zone (SVZ) of Chile (37–46°S) have experienced significant frontal retreats and area losses in recent decades which have been primarily triggered by tropospheric warming and precipitation decrease. The resulting altitudinal increase of the Equilibrium Line Altitude or ELA of glaciers has lead to varied responses to climate, although the predominant volcanic stratocone morphologies prevent drastic changes in their Accumulation Area Ratios or AAR. Superimposed on climate changes however, glacier variations have been influenced by frequent eruptive activity. Explosive eruptions of ice capped volcanoes have the strongest potential to destroy glaciers, with the most intense activity in historical times being recorded at Nevados de Chillán, Villarrica and Hudson. The total glacier area located on top of the 26 active volcanoes in the study area is ca. 500 km^2. Glacier areal reductions ranged from a minimum of -0.07 km^2 a^{-1} at Mentolat, a volcano with one of the smallest ice caps, up to a maximum of -1.16 km^2 a^{-1} at Volcán Hudson. Extreme and contrasting glacier–volcano interactions are summarised with the cases ranging from the abnormal ice frontal advances at Michinmahuida, following the Chaitén eruption in 2008, to the rapid melting of the Hudson intracaldera ice following its plinian eruption of 1991. The net effect of climate changes and volcanic activity are negative mass balances, ice thinning and glacier area shrinkage. This paper summarizes the glacier changes on selected volcanoes within the region, and discusses climatic versus volcanic induced changes. This is crucial in a volcanic country like Chile due to the hazards imposed by lahars and other volcanic processes.

1. Introduction

Most of the glaciological research which has taken place in Chile during recent decades has focused on the Patagonian Icefields (46.5–51.5°S) as they represent the main Chilean glacier contribution to sea level rise (Rignot et al., 2003). In contrast, the central-south Andes of Chile (33°-46°S), have been poorly studied (Rivera et al., 2002, 2008a,b). The great majority of the glaciers within this province, in the Southern Volcanic Zone (SVZ), are located on top of active volcanoes which can generate mudflows, lahars and pyroclast flows during eruptive events, having negative consequences on the population and infrastructure of nearby areas.

The most remarkable regional climate trend within the XXth century is the warming of upper (850–300 hpa) troposphere levels (Aceituno et al., 1993). This warming trend is however, strongly contrasted by the cooling in 1950's–1970's at stations between Concepción and Puerto Montt (Rosenblüth et al., 1997). In spite of this general trend, more recent studies have described a contrasting behaviour between low altitude stations, experiencing cooling or non significant temperature changes, and higher altitude stations exhibiting warming (Falvey and Garreaud, 2009).

Precipitation decreases in the region are more marked than temperature changes, with a maximum reduction at 39°S of 450 mm in the last 70 years (Bown and Rivera, 2007). This decreasing trend is at least partly explained by the El Niño Southern Oscillation events in the Southern Pacific Ocean (Montecinos and Aceituno, 2003), which have been more frequent and intense since the climatic shift of 1976 (Giese et al., 2002).

In response to these climatic trends, glaciers in the SVZ have undergone a generalized trend of frontal retreats (Masiokas et al., 2009), area losses (Rivera et al., 2012), negative mass balances (Rivera et al., 2005) and negative elevation changes (Rivera et al., 2006), resulting in significant contribution to sea level rise (Jacob et al., 2012), affecting water resources and increasing natural

* Corresponding author. Tel.: +56 63 234564; fax: +56 63 234517.
E-mail address: fbown@cecs.cl (F. Bown).

0895-9811/$ – see front matter © 2013 Elsevier Ltd. All rights reserved.
http://dx.doi.org/10.1016/j.jsames.2013.02.004

hazards. The observed rates of these changes are however very different for each glacier, depending on the topographic context, the type of glacier geometry, the presence of calving activity, the amount and characteristics of debris covering the ice, and certainly, the presence of volcanic activity near the glaciers (Rivera et al., 2008a; Warren and Aniya, 1999; Aniya et al., 1997).

Indeed, volcanic activity in the Southern Chilean Andes is crucial for explaining the behaviour of glaciers (total area almost 500 km^2) distributed on the tops and flanks of the 26 active volcanoes located between 36 and 37°S. In particular, those connected to a ~1000 km-long mega fault known as Liquiñe-Ofqui Fault Zone (LOFZ) extending from 39°S to 47°S (Lara et al., 2008). Impacts on glaciers are expected to be significant due to the occurrence of pyroclast debris and lava flows, tephra deposition, hot-rock avalanches (Trabant et al., 1994) and intense degassing (Major and Newhall, 1989). Hence, frequent eruptions of these ice-capped volcanoes during the XXth century have resulted in rapid snow/ice melting, ice crevassing, ice avalanches, superficial scouring or erosion, basal melting due to higher geothermal heat fluxes and substantial ice loss following eruptions (Fuenzalida, 1976).

Pyroclastic flows are much more effective than lava flows or ash fall, in producing large volumes of water during eruptions at ice-capped volcanoes (Major and Newhall, 1989; Thouret et al., 2007). In all cases however, when snow and ice located on volcanic edifices suddenly melts as a consequence of an eruption, large volumes of water descend along the volcanic flanks, initially as debris flows and later on, as hyper-concentrated and accelerated flows known as lahars (Cas and Wright, 1987). This type of mudflows could be dangerous (Newhall and Punongbayan, 1996), and they can have dramatic consequences for the population living nearby those volcanoes. An example is the lahar initiated by the 1985 eruption of Nevado del Ruiz in Colombia, which killed 23,000 people and injured more than 5000 (Voight, 1996; Thouret et al., 2007).

Volcanological studies in Southern Chile have focused on the geological, geochemical and flow dynamics characteristics of the main active volcanoes, their products and recent eruptive histories, effusion rates, pyroclastic flows, lava flow dynamics, mudflow deposits and associated volcanic hazards (Lara, 2004; Clavero and Moreno, 2004; Moreno, 2000). Nevertheless, the majority of the casualties arising from recent volcanic activity are due to lahars rather than other volcanic processes (e.g. Naranjo and Moreno, 2004), and therefore, the study of the water equivalent volume storage in the form of glaciers is highly necessary to mitigate this volcanic hazard (Castruccio et al., 2010).

In order to tackle this lack of comprehensive understanding of ongoing regional glacier changes, this paper aims to provide an overview of recent glacier variations of ice-capped active volcanoes in the southernmost province of the SVZ (37–46°S), in addition to discussing the incidence of climatic changes together with the effects of recent volcanic activity. With this purpose, this study includes a selected group of volcanoes in this province (see Table 1, Fig. 1) all of which are well documented in historical times and are partially ice-covered.

2. Methodology

A set of satellite imagery has been acquired (Table 1) which permits mapping of the ice-capped volcanoes at different dates using standard glacier extent classification procedures (Kargel et al., 2005). Other complementary datasets comprise topographic surveys and historical documents (Table 1) which extend the time series back to the mid-XXth century. Frontal and areal glacier changes were calculated by comparing all data sets using specialised software and digital techniques described below.

2.1. Remote sensing data: acquisition and pre-processing

Remote sensing data used in this paper are mainly visible medium resolution satellite imagery, namely Landsat Multi Spectral Scanner (MSS), Landsat Thematic Mapper (TM) and Enhanced Thematic Mapper (ETM+), as well as Advanced Spaceborne Thermal Emission and Reflection Radiometer (ASTER). These images were downloaded from the WIST-NASA web interface thanks to the GLIMS project (Kargel et al., 2013). The scene selection was based primarily on acquisition time, with preference given to images from

Table 1
Data sets used in the analysis of recent glacier changes.

Name	Lat. S/Long. W (decimal degrees)	Satellite data	Other data sets	Summit elevation (m a.s.l.)
Nevados del Chillán Volcanic Complex	36.85/71.36	MSS Mar 22, 1975; TM Mar 17, 1989; ASTER Mar 26, 2004 & Feb 19, 2011	SRTM 2000	3212
Volcán Callaqui	37.92/71.43	MSS Feb 13, 1975; ASTER Mar 27, 2011	OEA 1961; SRTM 2000	3164
Nevados de Sollipulli	38.97/71.52	TM Feb 16, 1990 & Mar 31, 2000; ASTER Mar 7, 2011		2282
Volcán Villarrica	39.41/71.93	MSS Feb 8, 1976; ASTER Feb 2, 2005 & Feb 24, 2007		2847
Volcán Mocho -Choshuenco	39.73/72.03	MSS Feb 4, 1976; TM Sept 2, 1987; ETM + Feb 25, 2011	OEA 1969; SRTM 2000	2422
Volcán Osorno	41.10/72.49	TM Feb 9, 1987; ASTER Feb 18, 2005	OEA 1961; SRTM 2000	2652
Volcán Michinmahuida	42.84/72.45	MSS Apr 23, 1979; ASTER Apr 4, 2007; Jan 1, 2009 & Feb 10, 2011	SRTM 2000	2404
Volcán Yanteles	43.52/72.82	MSS Mar 18, 1979; TM Jan 25, 1985; ASTER Apr 4, 2007	SRTM 2000	2042
Volcán Melimoyu	44.07/72.86	MSS Mar 14, 1976; TM Mar 26, 1986; ASTER Apr 4, 2007 & Jan 26, 2011		2400
Volcán Mentolat	44.69/73.07	MSS Feb 9, 1979; TM Mar 26, 1986; ASTER Apr 4, 2007; ETM + Apr 8, 2011		1660
Volcán Cay	45.06/72.99	MSS Feb 9, 1979; TM Mar 7, 1985,		2200
Volcán Macá	45.11/73.14	ASTER Apr 4, 2007; ETM + Apr 8, 2011		2960
Volcán Hudson	45.90/72.97	MSS Feb 9, 1979; TM Mar 3, 1985, Mar 8, 2000 & Mar 11, 2001; ASTER Mar 2, 2002; Feb 27, 2005 & Apr 4, 2007		1905

TM: Landsat Thematic Mapper; ASTER: Advanced Spaceborne Thermal and Reflection Radiometer; SRTM: Shuttle Radar Topography Mission; MSS: Landsat Multispectral Scanner; OEA Aerial photogrammetric survey; ETM+: Landsat Enhanced Thematic Mapper.

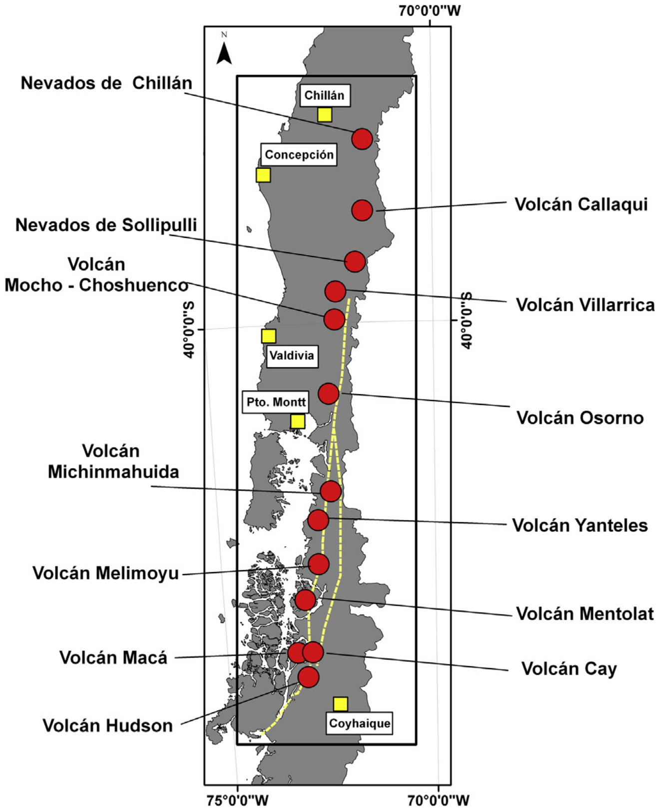

Fig. 1. Location map of the ice-capped volcanoes discussed in the text. The yellow lines represent the Liquiñe Ofqui mega fault (LOFZ). The inset box represents the Southern Volcanic zone (SVZ). Yellow squares represent main urban areas.

the end of summer, thus avoiding seasonal snow patches to permit discrimination between snow and ice (Kääb et al., 2003).

Orthometric correction and georeferencing of images was mainly based on Shuttle Radar Topography Mission (SRTM), 90 m pixel resolution data, and the satellite orbital parameters. The orthorectified Landsat MSS, TM and ETM + imagery were co-registered to ASTER data by using the Cosi-Corr software (Leprince et al., 2007) with subpixel error in co-registration between images. The full dataset was projected to Universal Transverse Mercator (UTM) zones 18S and 19S and datum WGS84. Data base management and analysis were carried out using Geographical Information Systems (GIS) tools from ENVISat and ArcMap.

2.2. Image glacier classification

Glacier extent classification procedures and band ratio segmentation were utilised, including the generation of false-colour composites derived from visible and/or near infrared bands (Landsat bands 5-4-3 or 5-4-1 and ASTER 3-2-1). Using histograms, adjusted by different threshold values, an accurate glacier classification was obtained. The best results were obtained with Landsat TM4/TM5 and ASTER VNIR 3/SWIR 4 band ratioed images (Kargel et al., 2005). Furthermore, manual on-screen editing, essentially a manual smoothing, was performed to reduce the fractal structure along glacier boundaries (Rivera et al., 2006). Another applied classification used scatterplots of ASTER VNIR1/VNIR 3 band ratios (Kargel et al., 2005) to define facies (snow, bare ice, ash-covered areas, etc), based upon the maximum likelihood technique. Albedo changes of snow/ice facies due to volcanic ash deposition were analysed with VNIR ASTER data.

2.3. Aerial photographs, cartography and other data processing and analysis

Vertical photographs and cartographic data (Table 1) from the 1960s extended the analysis to several decades for some glaciers. Photograph pairs were digitised by high-resolution scanners and then geo-referenced to UTM WGS1984 datum, with tie points identified in the photos and cartography. Further processing was carried out with the Microstation 8 Terraphoto module and Erdas Imagine 8.4. Glacier outlines were digitised over a stereoscopic model of nominal scale depending on flight altitude, making them comparable to the satellite-derived polygons obtained using the GIS tools mentioned above.

Former glacier inventories based on aerial photographs and field studies (Rivera, 1989), and other documentary records such as terrestrial photography or historical accounts (Phillippi, 1862) and oblique aerial photographs (TRIMETROGON from 1944/45) have in some cases been interpreted together with the rest of the data. Data on volcanic eruptions have been derived from a number of sources as described below for each volcanic complex.

2.4. Determination of surface changes and associated errors

Glacier area and frontal change were calculated by arithmetically comparing polygons and lines obtained for each date. Net values were averaged over different time intervals in order to extract annual rates ($km^2\ a^{-1}$ or $m\ a^{-1}$). Special attention was given to periods before and after eruptive events, where ice variation patterns were compared to the geological record of each eruption.

A systematic horizontal error was assumed according to the method described in Rivera et al. (2007), where the pixel size is multiplied by the perimeter of the changing portion and annually averaged by the time interval. The vertical error is a function of topographic data, which is on the order of $\sim$10 m (Rivera et al., 2006).

3. Geological and volcanological setting

The main tectonic feature of the SVZ is the intra-arc Liquiñe-Ofqui fault zone or LOFZ, having two NNE-trending right-stepping straight alignments extending more than 1000 km through plutonic rocks of the North Patagonian Batholith (Cembrano et al., 1996), which is characterized by the presence of low grade metamorphic complexes although having different units well defined east and west of this Mesozoic to Cenozoic batholithic belt (Hervé et al., 2007). The LOFZ is a long-lived shear zone from the convergence of the Nazca and South American plates (Hervé et al., 2009), whose present-day activity is well reflected on seismicity records (Lange et al., 2008). The regional volcanoes are spatially associated with the LOFZ, which controls magma rise and the volcanic emplacement. Tectonics-volcanism interplay has indeed been of major concern in the SVZ, where two main categories of association are i) the current dextral transpressional tectonic regime, characterized by primitive magmas along NE-trending stratovolcanoes and monogenetic cones, and ii) stratovolcanoes exhibiting more evolved terms and built on top of ancient reverse and strike–slip faults of the LOFZ (Cembrano and Lara, 2009).

Knowledge of the relationship between crustal stresses beneath Andean arc volcanoes and pre-eruptive crystallization and magma residence times is so far, moderate. Isotopical analysis, however, suggests recent material alteration involved in magma petrogenesis and volcano loading impacts on subvolcanic weathering processes (Zellmer et al., in press). Geochemical and tectonics criteria have provided bases for recognition of several provinces based on volcanic alignment and the products mineralogy and petrography.

The central (CSVZ 37–41°30′S) province for instance, is characterized by basalts to basaltic andesites, where NE and NW alignments of strato-volcanoes are typically observed. The south (SSVZ 41°30′-46°S) province is comprised of two basalt types i.e. normal andesites-dacites and mixed andesite-dacites and scarce rhyolites, with stratovolcanoes aligned NE (López-Escobar et al., 1995). In conjunction, the CSVZ and SSVZ (37°–46°S) accounts for tens of volcanic eruptions in historical and Quaternary times (Stern, 2004). This record is well documented in Simkin and Siebert (2002) and reveals diverse eruption types, timings and explosive levels. In order to represent this wide range of volcanic activity, we have selected 13 ice-capped volcanoes located from 37°S to 46°S.

Among very active ice-capped volcanoes are:

The *Nevados de Chillán volcanic complex* (36.85°S/71.36°W), a composite stratovolcano of Late Pleistocene-to-Holocene age having polygenic characteristics, lava domes and several parasitic cones. The two main eruptive subcomplexes are the Cerro Blanco/Volcán Gertrudis to the NW (maximum altitude of 3212 m a.s.l.), with the existence of several volcanic units (Mee et al., 2009), and Las Termas (Volcán Nuevo/Volcán Chillán/Volcán Arrau) to the SE (maximum altitude of 3206 m a.s.l.). These subcomplexes are separated by the Portezuelo Los Baños and have evolved differently along the past 40 ka (Naranjo et al., 2008).

In this moderately ice-covered volcanic complex, signs of historical activity are recorded since the early 18th century (González-Ferrán, 1995). Volcán Santa Gertrudis erupted in 1861–65 producing basaltic-andesitic to andesitic materials (Philippi, 1862) that are widely spread down Cerro Blanco subcomplex (Fig. 2 left), whilst Volcán Nuevo has been building up since the 1906 eruption (Brüggen, 1950). A new cone was formed between Volcán Nuevo and Arrau in August–September 2003 (Naranjo and Lara, 2004) obliterated by the growth of these volcanoes in 1906–1943 and 1973–1986, respectively (Naranjo et al., 2008). This active volcanic complex is located in an economically dynamic region characterised by prominent agriculture, mining and tourism industries, therefore its eruptive history and hazardous nature have been of major interest (Dixon et al., 1999; Mee et al., 2006). The historical record has been recently compiled by, among others, Petit-Breuilh (1995).

Volcán Villarrica (39.41°S/71.93°W) is a stratocone characterized by mild strombolian activity (Lara, 2004), permanent degassing and periodic explosions within the main crater, which may be considered as a hazard to climbers (Witter and Delmelle, 2004). The crater contains a lava lake, which has remained at a high level (90–180 m below the crater rim) and is very sensitive to the magmatic conduit activity (Calder et al., 2004; Witter et al., 2004). The historical record indicates frequent moderately explosive eruptions since 1558 (Petit-Breuihl and Lobato, 1994).

Unlike the Chillán complex, the significance of a larger glacier cover results in the interaction with lavas in turn generating lahars during eruptions in 1948–1949, 1963–1964, and 1971–1972 which resulted in the death of more than 75 people (Stern, 2004). This is considered the main hazard of the volcano (Moreno, 2000). In the most recent of these eruptions, lahars descended at 30–40 km h^{-1} towards Lagos Villarrica and Calafquén (Naranjo and Moreno, 2004) after lavas from a NNE fissure on the upper flanks of the volcano melted the glacier cap (Naranjo and Moreno, 2004).

Volcán Hudson (45.90°S/72.97°W) is an active stratovolcano with a 10 km diameter caldera and an estimated area of 75 km^2 (Gutiérrez et al., 2005). Due to its remoteness and unpopulated location in the Aysén region, it was only recognized as an active volcano in 1970 (Fuenzalida and Espinosa, 1974). More than 10 Holocene eruptions have been identified, with the eruption calibrated to 6700 BP as the largest ever recorded in the Southern Andes (Stern, 1991). The Hudson caldera is thought to have been generated during one of these large Holocene eruptions (Naranjo and Stern, 1998), however Orihashi et al. (2004) proposed that it was formed by multiple collapsing events.

In recent historical times, Hudson has experienced two plinian eruptions, one in August and September of 1971, with the plume reaching an altitude of 12,000 m, and the other in 1991, which produced >4 km^3 bulk volume of tephra, affecting an area of more than 150,000 km^2 in Chile and Argentina, been detected even in Antarctica ice core records (Legrand and Wagenbach, 1999). In the latter event, a phreatomagmatic eruption first occurred in the NW corner of the caldera (Kratzmann et al., 2009), revealing the importance of the ice volume storage in triggering this phase. Together, the geological record and collection of satellite imagery, illustrate a dynamic recent history of ice shrinkage/destruction during both eruptions (Branney and Gilbert, 1995). Both events caused several lahar flows at the Río Huemules and had severe economic and social impacts, especially due to continuing ash storms afterwards (Wilson et al., 2011). Thanks to the use of Interferometric Synthetic Aperture Radar (InSAR), Pritchard and Simons (2004) detected surface deformation associated with magmatic processes at Volcán Hudson, where an inflation of near 5 cm/yr followed the 1991 eruption, which was reduced to a more recent rate of 2 cm/yr between 2004 and 2008 (Fournier et al., 2010).

Other active volcanoes of the SVZ have also undergone explosive eruptions in the XX and XXI centuries, such as Quizapu in 1932 (Hildreth and Drake, 1992), Cordón Caulle in 2011 (Singer et al.,

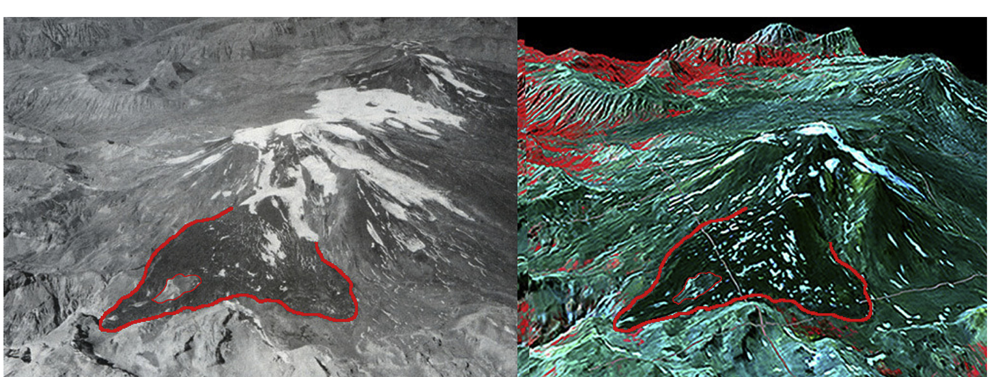

Fig. 2. Nevados de Chillán Trimetrogon aerial photograph of 1944/45 (left), compared to a 3D representation of an ASTER image of the same area collected in February 19, 2011. In red is delineated the Santa Gertrudis lava flow from the 1861 eruption described in the text. The glacier described in the text as located between the two main volcanic cones, called Portezuelo de los Baños, was totally gone by 2011.

2008), and Volcán Chaitén, which in May 2008 began a sequence of eruptions and high altitude-ejection of gases followed by lava dome effusions and extremely hazardous pyroclast flows (Carn et al., 2009). Although evidence for a long dormant period had been strong pre-eruptive seismic warning in 2008 was extremely short due to the very rapid rhyolite magma ascent through the sub-volcanic system (Castro and Dingwell, 2009). The result was that the finest ashes reached the coast of Argentina and the bulk tephra volume was estimated in 0.5–1 km^3 (Alfano et al., 2010).

Among historically less active ice-capped volcanoes are included:

Volcán Callaqui (37.92°S/71.43°W), an elongated and eroded cone composed by andesitic and basaltic lavas (González-Ferrán, 1995) with minor sulfataric and fumarolic recent activity (Radic, 2010).

Volcán Mocho-Choshuenco (39.73°S/72.03°W), a volcano characteristic by a central depression and two main peaks, whose last known eruption dates from 1864 due to which it is considered a dormant complex without eruptive activity (Rodríguez et al., 1999). Another volcano with moderate activity is *Osorno* (41.10°S/72.49°W), which underwent enhanced eruptive cycles and phreatomagmatic explosions along the 1800s and whose last event was recorded in 1869 (López-Escobar et al., 1995).

Volcán Michinmahuida (42.84°S/72.45°W) a Pleistocene to Holocene stratovolcano/caldera elongated 14 km in a northeast-southwest direction. Late Holocene tephra deposits are well recognised at the shores of Lago Futalafquén, in Argentina (Naranjo and Stern, 2004). Prominent eruptions took place in 1742 and later on in 1834 (González-Ferrán, 1995). Volcán Chaitén, which is non-ice covered, is located few km to the west (Fig. 4). As a result of the 2008 eruption, a thick layer of ashes were deposited on top of Michinmahuida glaciers (Watt et al., 2009), producing a drastic reduction in surface albedo (Rivera et al., 2012).

Volcán Mentolat (44.69°S/73.07°W) is an ice-filled 6 km-caldera. Petrography and geochemistry of this center is characterised by basaltic andesites commonly containing plagioclase + clinopyroxene + orthopyroxene ± olivine phenocrysts. Although there is activity reported back to 7000 BP, with the production of pumice and scoria layers, the best preserved deposits date from an eruption recorded at the beginning of the XVIII century, which generated lava flows west of the volcano.

Several *Holocene volcanoes* remain inactive at present like;

Nevados de Sollipulli (38.97°S/71.52°W), a well preserved 4 km-diameter approximately circular volcanic caldera of Plio-pleistocenic age is located between the two most active volcanoes of the SVZ (Villarrica and Llaima). Its record is substantially different, with the last eruption at 700 years BP (Gilbert et al., 1996) and an explosive eruption ca. 2900 BP, known as Alpehué, which was triggered by the ascent of andesitic-basaltic magma to the upper magma chamber where it mixed with silicic material. As described by the Smithsonian Global Volcanism program (http://www.volcano.si.edu/index.cfm), the caldera may have a non-explosive origin but eruptions in the following have been focused on its walls which have increased in height, yielding as a potential dangerous volcano.

Further south, in Continental Chiloé (~42°–45°S), the late Cenozoic LOFZ displacement generated deep pull apart basins to the West. An extended rhyolitic volcanic field developed in Miocene times and later on, graniodiorite plutons and Holocene andesite-basalts stratovolcanoes were aligned to the LOFZ. This feature has been of major influence on the tectonic evolution of the area (Pankhurst et al., 1992).

One of these stratovolcanoes is *Volcán Yanteles* (43.52°S/72.82°W), which shows strong stratigraphic evidence for medium to large eruptions in Holocene times (Naranjo and Stern, 2004). Then *Volcán Melimoyu* (44.07°S/72.86°W) a stratovolcano with a 1 km diameter crater (Naranjo and Stern, 2004), is characterised by four summits which have mainly been constructed by phreatomagmatic eruptions in the Late Holocene. *Volcán Macá* (45.11°S/73.14°W) is comprised by a caldera and monogenetic pyroclast and lavic domes in a fissure developing NE-SW (González-Ferrán, 1995). Pumice tephra deposits along the valleys of Ríos Simpson and Mañiguales (~70 km) were dated at 1540 BP (Naranjo and Stern, 2004) and so far stands as its last known eruption. Magmas at Macá are not significantly affected by crustal contamination but by crystal fractionation, which is consistent with the thin and young crust under this volcano (D'Orazio et al., 2003). Finally, *Volcán Cay* (45.06°S/72.99°W), a highly eroded stratovolcano, shares similar petrogenetic characteristics to Volcán Macá but has a different record (D'Orazio et al., 2003). Some authors such as González-Ferrán (1995) suggests a Holocene-to-recent age for numerous parasitic monogenetic basaltic cones aligned within a fracture that forms part of the LOFZ.

4. Glacier changes

4.1. Most active ice-capped volcanoes

4.1.1. Nevados de Chillán volcanic complex (36.85°S/71.36°W)

The first recorded descriptions of the area are ascribed to Domeyko in 1848 and Philippi in 1862 who described "*a powerful bank of ice*" at Portezuelo de los Baños (Brüggen, 1950). Philippi (1862) produced a map, which, when compared to present cartography, indicates a severe reduction in ice area over the last 150 years. In 1944/45, the first oblique TRIMETROGON aerial photograph (Fig. 2 **left**) showed a glacier which compared to the sketch map of 1862, seems to be much smaller. The glacier ice in 1975, when one of the first vertical aerial photographs was taken, was estimated to be 15.8 km^2, mainly concentrated at the NW subcomplex, which is considered to be a less active vent (Simkin and Siebert, 2000). In 2011 (Fig. 2, **right**), there are still some small remnants of the former glacier at the Portezuelo Los Baños, and the remaining small ice bodies have become dominantly ash/debris-covered. Between 1975 and 1989, the glacier area suffered a significant reduction, coinciding with the eruption between 1973 and 1986 of a new cone baptized as Volcán Arrau (Dixon et al., 1999).

Accompanying the general area shrinkage, the number of individual ice bodies (whether glaciers or glaciarets) increased from 31 to 40 in the period following the 2003 eruption (2004–2011). By extending the analysis up to the most recent ASTER image acquired in 2011, the annual area reduction since 1975 is 0.36 km^2 a^{-1} (Table 2).

4.1.2. Volcán Villarrica (39.41°S/71.93°W)

Based on the ASTER 2007 satellite image, the volcano glacier area yielded ~30 km^2 (Table 2), indicating a total reduction of more than 20% since 1961. Large volcanic events took place in 1964 and 1971, however larger glacier area changes were concomitant to a volcanic cycle between the '70s and '80s characterised by four eruptions (1977, 1980, 1983 and 1985). In this period, a large volume of fumarolic and eruptive materials was ejected, producing several lahars descending the volcanic flanks (Clavero and Moreno, 2004).

Frontal variations of the main outlet glacier flowing towards the south-east, Pichillancahue-Turbio (16.78 km^2 in 2007), a partially ash/debris-covered ice tongue infilling the volcanic caldera depression, has a negative trend of 30 m a^{-1} between 1961 and 2007 (Table 3), also with significant ice thinning in recent decades (Rivera et al., 2006).

4.1.3. Volcán Hudson (45.90°S/72.97°W)

Fuenzalida (1976) estimated that 80% (approximately 60 km^2) of the ice within the Hudson caldera was destroyed or melted during the

Table 2
Glacier areas at ice-capped volcanoes studied in this work and interdecadal areal loss trends. Numbers of glacier basins delineated at each volcano and studied in this work are indicated.

Name	(Year) number studied glaciers	(Year) Glacier area in km^2					Glacier area change (km^2 a^{-1})	Period
		'60s	'70s	'80s–'90s	2000–2005	>2005		
Nevados del Chillán	(2011) 39 (2004) 26		(1975) 15.80	(1989) 7.90	(2004) 5.30	(2011) 2.73	−0.36	1975–2011
Volcán Callaqui	(2011) 13	(1961) 14.10	(1975) 13.60			(2011) 7.17	−0.14	1961–2011
Nevados de Sollipulli	(2011) 2	(1961) 19.07		(1990) 13.67	(2000) 12.81	(2011) 11.46	−0.15	1961–2011
Volcán Villarrica	(2011) 4	(1961) 39.91				(2007) 30.01	−0.21	1961–2007
Volcán Mocho-Choshuenco	(2011) 8	(1969) 27.66	(1976) 27.40	(1987) 23.07		(2011) 17.72	−0.24	1969–2011
Volcán Osorno	(2011) 6	(1961) 10.88		(1987) 7.80		(2005) 5.60	−0.12	1961–2005
Volcán Michinmahuida	(2011) 9		(1979) 93		(2007) 81.83	(2011) 75.66	−0.54	1979–2011
Volcán Yanteles	(2011) 24		(1979) 66.39	(1985) 61.27		(2007) 46.24	−0.72	1979–2007
Volcán Melimoyu	(2011) 7		(1976) 69.57	(1986) 59.88	(2007) 57.03	(2011) 55.59	−0.40	1976–2011
Volcán Mentolat	(2011) 9		(1979) 5.62	(1986) 4.17	(2007) 3.56	(2011) 3.35	−0.07	1979–2011
Volcán Cay	(2011) 8		(1979) 9.05	(1985) 6.66	(2007) 5.77	(2011) 5.81	−0.10	1979–2011
Volcán Macá	(2011) 18		(1979) 45.08	(1985) 37.17	(2007) 31.17	(2011) 27.62	−0.54	1979–2011
Volcán Hudson	(2008) 1		(1979) 92.08	(1985) 90.79	(2002) 71.13	(2007) 69.84	−0.79	1979–2007

1971 eruption. In 1979 the ice seemed to have recovered, because the caldera was almost totally ice covered, and together with the ice tongues leaving the caldera (Glaciar Huemules), the total ice area had increased to 92 km^2. By the mid-1980s, Glaciar Huemules' area had remained almost unchanged (90.8 km^2), with an estimated total ice volume of 2.5 km^3 within the caldera (Naranjo and Stern, 1998). But once again, the 1991 eruption melted/destroyed 20 km^2 of the ice within the caldera, as derived from an ASTER image acquired in 2002. At this time it was possible to see new cones within the caldera in areas previously covered by ice, but now surrounded by small lagoons between concentric ice crevasses, indicating that melting water produced due to the geothermal heat flux coming from these new eruptive centres is flowing concentrically around the cones, and not as used to be, toward the main glacier tongue (Huemules) leaving the caldera rim on the western flank.

Glacier Huemules' total area in 2002 was 71.13 km^2, indicating an area reduction rate of 1.16 km^2 a-^{1} since 1985. During the years which followed (2002–2007), the glacier within the caldera experienced some gains in areas destroyed by the 1991 eruption, however, Glaciar Huemules as a whole experienced a small area shrinkage (1.29 km^2 in 5 years), mainly explained by the frontal retreat and area lost near its frontal debris covered tongue (Table 3). This debris-covered area is the result of lahars flowing over the surface and sides of Glaciar Huemules during the 1971 (Fuenzalida, 1976) and 1991 (Branney and Gilbert, 1995) eruptions.

Recent satellite imagery reveals the contrasting morphology that the glacier may adopt before and after eruptive events. In years preceding the volcanic activity reported in October 2011, Huemules' tongue remained densely debris-covered but dirty snow was only visible at the central part of the caldera. This subglacial eruption generated minor eruptive columns and concentric crevasses surrounding the coalescence of the three craters of the caldera (Romero, 2012), where a thick layer of ash is observed at the end of 2011. In addition, lahars were reported as descending from several valleys down the caldera. Early-mid summer 2011–2012 was particularly warm and dry in southern Chile according to Boletín Climático of Geophysics Department, U. of Chile (http://met.dgf.uchile.cl/clima/), which strikingly, considers December 2011 as the driest month of December within the last 10 years. Based on this, reduced seasonal snow is expected as a consequence of the widespread tephra layer being exposed by the end of summer 2012.

Table 3
Frontal changes of selected glaciers.

Volcano/Glacier tongue	Frontal change (m)	Frontal change rate (m a −1)	Period
Nevados del Sollipulli/Alpehué	−1350	−27	1961–2011
Volcán Villarrica/Pichillancahue	−1380	−30	1961–2007
Volcán Michinmahuida/Amarillo	−1804	−82	1979–2011
Volcán Melimoyu/Melimoyu Sur	−1120	−32	1976–2011
Volcán Hudson/Huemules	−1100	−50	1979–2007

4.2. Historically less active ice-capped volcanoes

4.2.1. Volcán Callaqui (37.92°S/71.43°W)

The earliest Volcán Callaqui glacier area, estimated to be 14.10 km^2, was obtained from aerial photos acquired in 1961 (Rivera, 1989). In the 1970s, no significant changes took place with a measured area of 13.60 km^2 in 1975, however by 2011 nearly 50% of the original area was lost. The annual rate of change between 1961 and 2011 was 0.14 km^2 a^{-1} (Table 2).

4.2.2. Volcán Mocho-Choshuenco (39.73°S/72.03°W)

A stake network deployed since 2003 in the southeastern glacier of the volcano was used to determine an annual mass balance of −0.88 m w.e. (meters of water equivalent) in the year 2003/2004 (Rivera et al., 2005), whereas a +0.36 m w.e. value resulted in the following year (Bown et al., 2007); with the difference attributed to the interannual precipitation and temperature variability. Biological analysis of snow/firn layers collected from a core in the accumulation area of the glacier, indicated similar annual accumulation rates. A wide range of measurements have been derived from this volcano, including crevasse detection, ice thickness surveys and ice elevation changes (Rivera et al., 2006).

The glacier variations of Volcán Mocho resulted in a 17% loss of ice area between 1976 and 2005 (Rivera et al., 2006), with evidence of accelerated loss since 1987. In contrast, ice elevation changes are not significant when compared to nearby Volcán Villarrica, where a strong negative signal has been found, potentially due to geothermal activity beneath the volcanic edifice (Rivera et al., 2006). Based on the most recent ASTER image (2011), Volcán Mocho has a glacier area of 17.72 km2 (Table 2), which implies an areal reduction of −0.24 km^2 a-^{1} since 1969, or a net reduction of 36% of the original area.

4.2.3. Volcán Osorno (41.10°S/72.49°W)

This volcano presents a glacier cover distributed over five main ice basins. The inventory of Rivera (1989) provides the oldest glacier data, based on which the 1961 area was 10.88 km^2.

A Landsat image was acquired in 1987, where the glacier area was estimated to yield 7.80 km^2 and an ASTER image collected in 2005 provided an estimate of 5.60 km^2 (Fig. 3). A trend of -0.12 km^2 a^{-1} is thus obtained over the whole period (Table 2).

4.2.4. Volcán Michinmahuida (42.84°S/72.45°W)

The glacier inventory at Michinmahuida yielded a total area of 75.66 km^2 of ice distributed among 9 glacier basins in 2011. A Landsat image of 1979 provided a glacier area of ca 93 km^2, yielding a 18% decrease in glacier area in 32 years (Table 2). A large frontal retreat has been observed, especially at Glaciar Amarillo between 1961 when the first vertical aerial photograph was obtained and 2007 (Table 3).

However, Rivera et al. (2012) described that Glaciar Amarillo experienced a significant advance of 240 m a^{-1} since November 2007, which persisted until early 2009, coinciding with the nearby eruption of Volcán Chaitén. An update of the frontal glacier variations between 2009 and 2011, after the eruption was over, revealed that the glaciers retreated again, following historical retreat rates (-72 m a^{-1} for Glaciar Amarillo and -152 m a^{-1} for Glaciar Noroeste). Rivera et al. (2012) also estimated a substantial thinning at the lower parts of the icecap, indicating a possible dynamic response to subglacial geothermal fluxes.

4.2.5. Volcán Mentolat (44.69°S/73.07°W)

The caldera was partially covered with a glacier of 3.35 km^2 in 2011. Between 1979 and 2011, the glacier reduction was almost 40% of its 1979 size with a rate of -0.07 km^2 a^{-1} (Table 2).

4.3. Holocene volcanoes

4.3.1. Nevados de Sollipulli (38.97°S/71.52°W)

The volcano was covered by a prominent (6 km^3) ice body with more than 600 m of ice thickness as measured in 1992, mostly

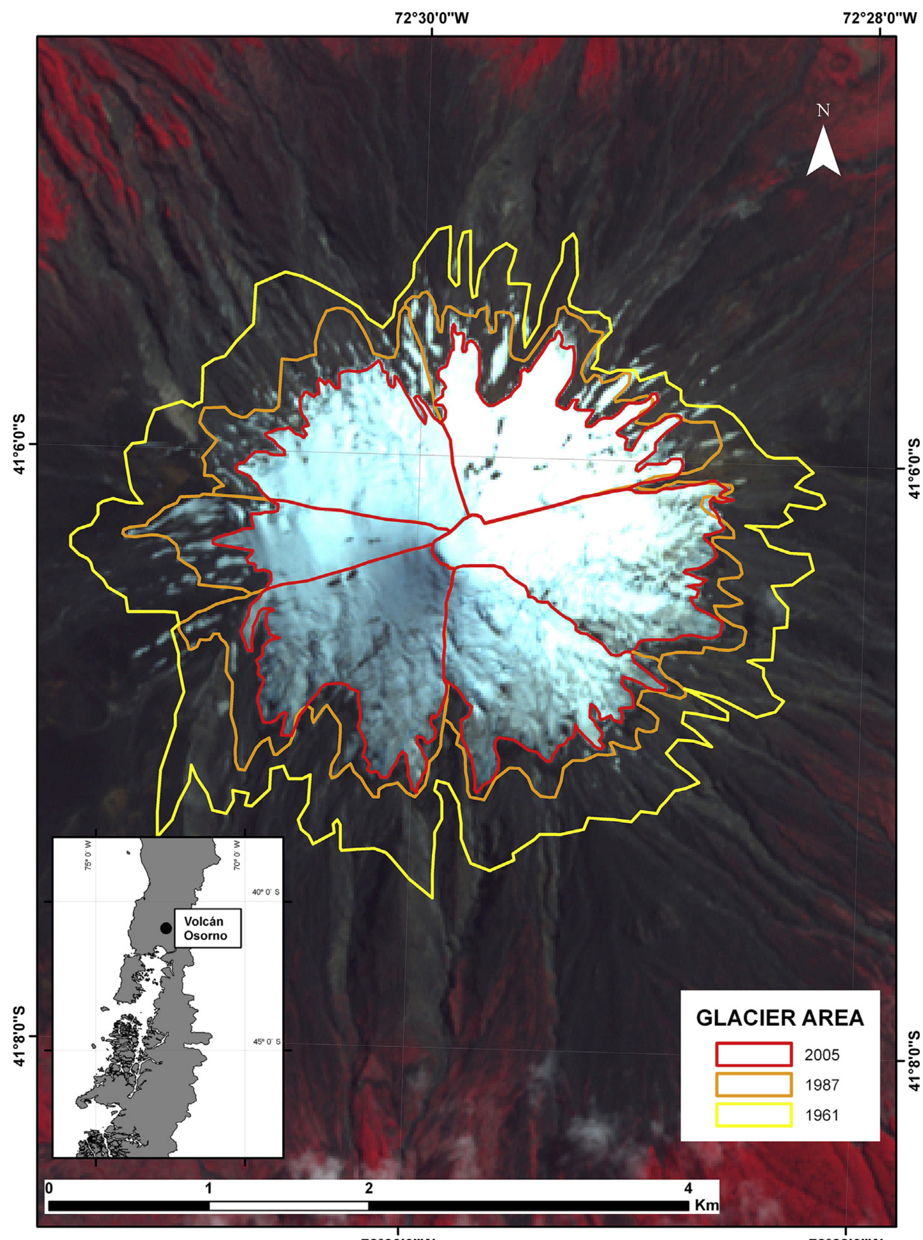

Fig. 3. Volcán Osorno glacier area 1961–2005. Ice divides are delineated in red. The background image is an ASTER false colour composite (3-2-1) from February 18, 2005.

within the caldera, and one ice tongue (Alpehué) flowing out of the caldera rim towards the south (Gilbert et al., 1996). According to aerial photographs from 1961, the ice covering the caldera was 19.07 km^2 (Rivera, 1989). The glacier net reduction between 1961 and 2011 was 7.61 km^2 (Fig. 4, Table 2). A frontal retreat of 1.3 km was also detected at the Alpehué valley between 1961 and 2011 (Table 3).

4.3.2. *Volcán Yanteles (43.52°S/72.82°W)*

The glacier capping the volcano was estimated to be 46.24 km^2 in 2007 (Table 2), and therefore is one of the largest ice surfaces in the area of Chiloé Continental. Between 1979 and 2007, the glacier reduction was -0.72 km^2 a^{-1}, and although maintaining the strong trend across the SVZ it is uncertain if this shrinkage has taken place monotonically during this 28 year-period.

4.3.3. *Volcán Melimoyu (44.07°S/72.86°W)*

Volcán Melimoyu has the greatest ice area in the region between 43° and 46°S totalling 55.59 km^2 in 2011. Between 1976 and 2011, the net glacier area reduction was 13.98 km^2 (Fig. 5, Table 2). The individual glacier with largest changes is Glaciar Anihue, which was reduced in area by nearly 4 km^2 in the same period. Another glacier, Melimoyu Sur, receded ca 1 km (Table 3) allowing the formation of a proglacial lagoon which is clearly visible in recent ASTER images.

4.3.4. *Volcán Cay (45. 06°S/72.99°W)*

The total inventoried ice in 2007 was 5.81 km^2. The net reduction since 1979 was estimated to be -0.10 km2 a^{-1} (Table 2) with a total reduction of 36% of its original area, which is a similar magnitude to the nearby Mentolat glacier reduction.

4.3.5. *Volcán Macá (45.11°S/73.14°W)*

A large area of ice extends across the volcanic complex, which, based on the ASTER image from 2011, has a total area of 27.62 km^2. Since 1979, the ice area experienced an areal reduction of -0.54 km^2 a^{-1} (Table 2) with a total loss of 38%.

5. Climatic vs volcanic factors on glacier changes

Although the glaciers in the studied region exhibited some differences, the great majority have experienced a receding trend over the last 50 years (Fig. 6). Prominent glacier changes have also

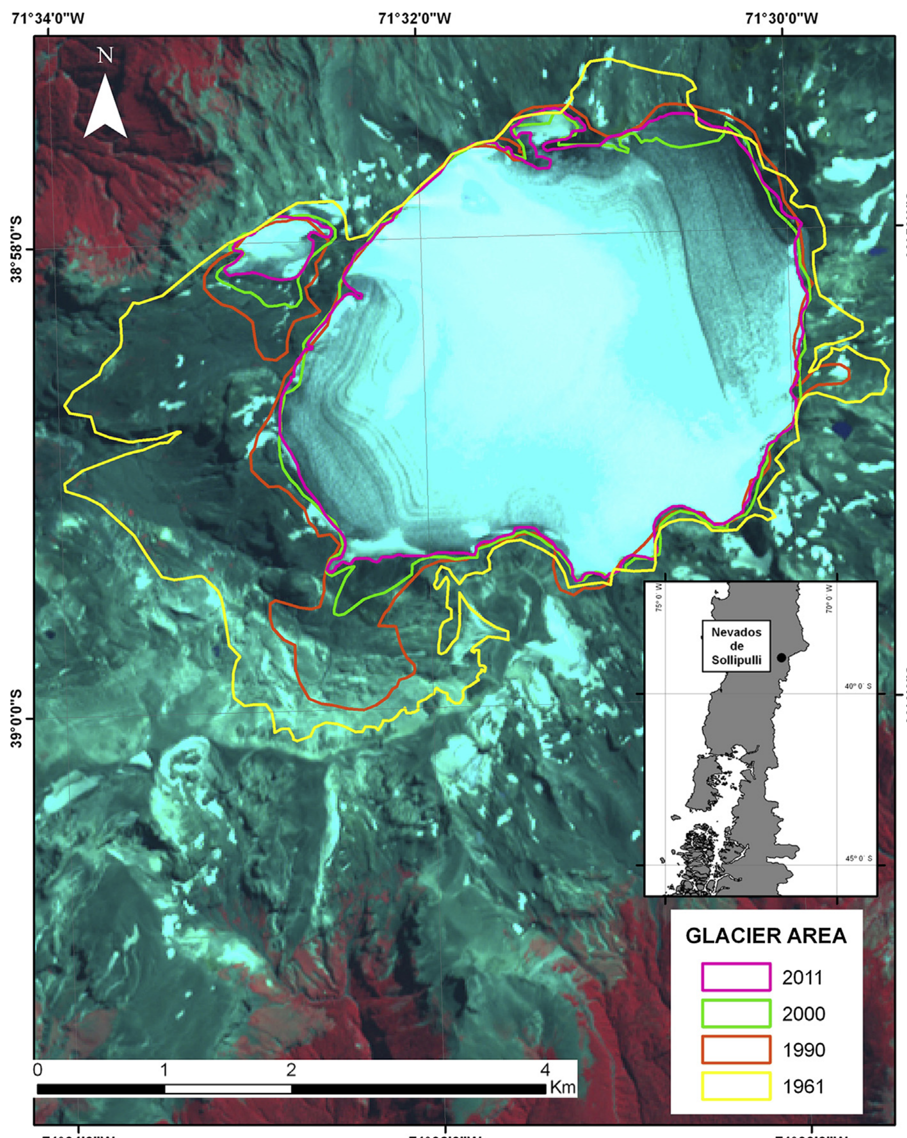

Fig. 4. Nevados de Sollipulli glacier area 1961–2011. The background image is an ASTER false colour composite (3-2-1) from March **7**, 2011.

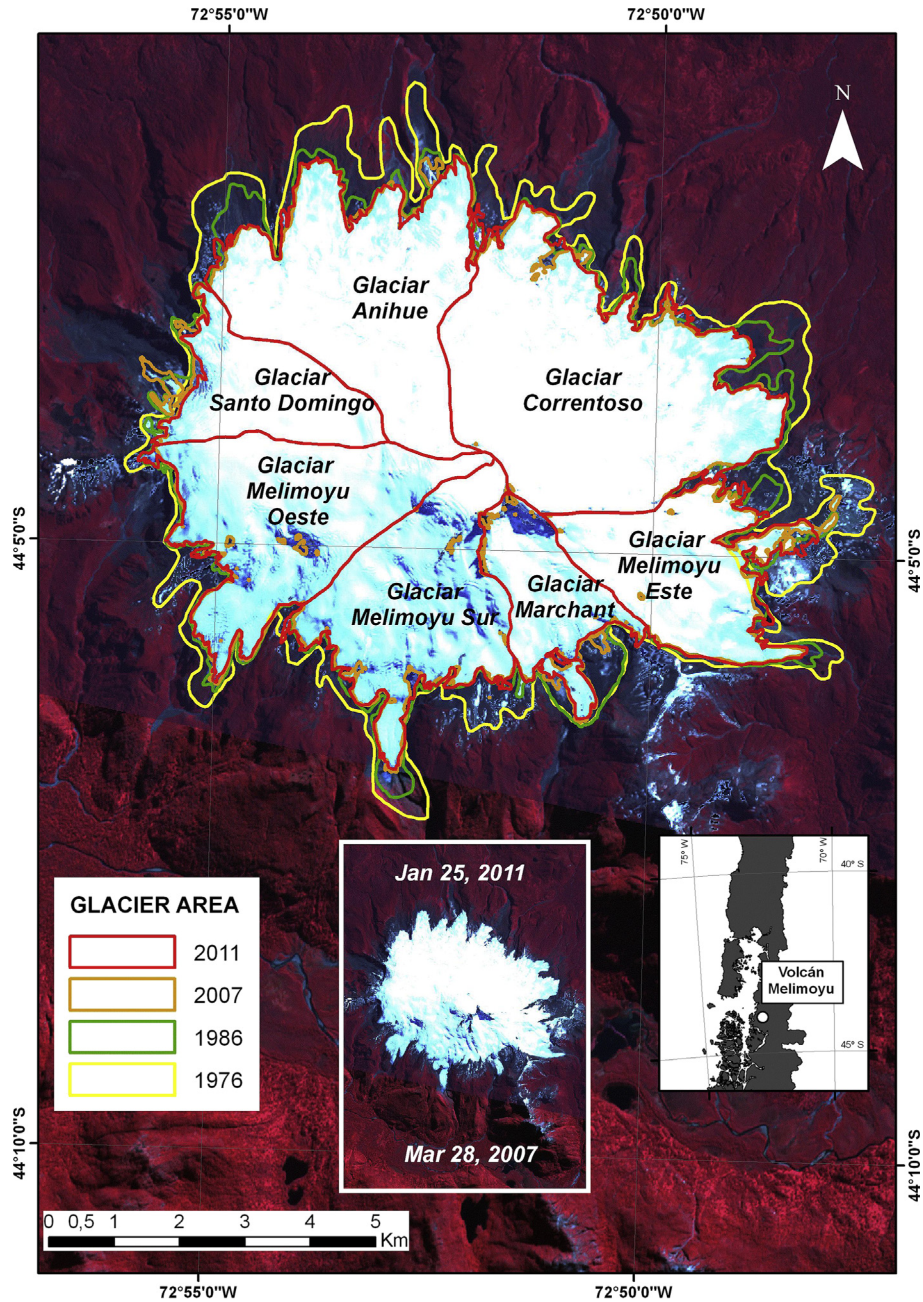

Fig. 5. Volcán Melimoyu glacier area 1976–2011. The background image is comprised of two ASTER false colour composites (3-2-1) from March 28, 2007 and January 25, 2011.

been connected to ice-capped volcanoes where explosive eruptions or volcanic cycles of several years have occurred during recent decades, i.e. Chillán, Villarrica and Hudson. The most important eruptive events are indicated in Fig. 6.

Overall, ice-capped volcanoes of the region have primarily responded to climatic change driving forces taking place in the region characterized by tropospheric warming in Northern and Central Chile (Falvey and Garreaud, 2009) and temperature increase detected at the 850 gpm level at Puerto Montt radiosonde station (40°S) between 1958 and 2000 (Bown and Rivera, 2007). These increases were highly influenced by the "1976 shift", because in the years before and after it, air temperatures showed no significant trends (Falvey and Garreaud, 2009). This is confirmed by an updated compilation of Puerto Montt radiosonde annual temperatures at 1500 m, which revealed no further increases between 2000 and 2010 (Fig. 6). This connection to the 1976 shift is at least partially explained by the Antarctic Oscillation Index (AOI), with positive values recorded around 1976 and since 1988. The low altitude stations in the region showed a contrasting trend, with little warming in the northern part (36°S Chillán to 39°S at Osorno), and no significant trends further south (Falvey and Garreaud, 2009).

With respect to precipitation, between 1930 and 2001 the number of rainfall days decreased in the whole study area, in addition to the rainfall reduction trend of 5–15 mm a^{-1} observed at the western flank of the Chilean Andes between 36 and 46°S (Carrasco et al., 2008), and in the eastern side of the Andes (Argentina) where a smaller but significant reduction in precipitation was also detected. The annual precipitation and its reduction in recent decades along these latitudes are well correlated

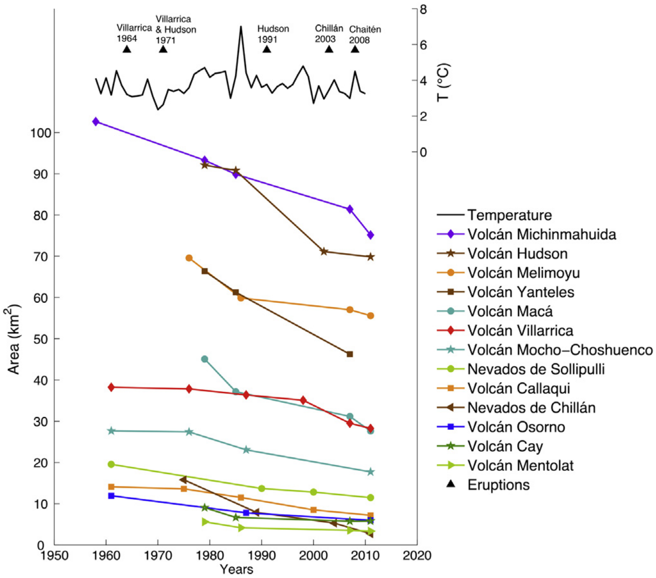

Fig. 6. Compilation of glacier variations since the 1960s of 13 ice-capped volcanoes studied in this work. Yearly-mean temperatures in 1958–2010 at 1500 m at Puerto Montt radiosonde station (41°S) are represented as a solid black line. Main volcanic eruptions are represented by black triangles.

(between −0.5 and −0.73) with the AOI, confirming the predominant influence of the contrasting baroclinic fields between Antarctica and the South Pacific region. In spite of this good correlation, a high inter-annual variability has been detected in the studied stations (Bown and Rivera, 2007). Recent studies show the negative rainfall trend still persists in the region from 37°S to 43°S, with decrease values between −2%/decade to −5%/decade in 1950–2007 (Quintana and Aceituno, 2012).

In the long-term, these rainfall reductions, in combination with upper atmosphere warming, have yielded an altitudinal increase in the whole region of the Equilibrium Line Altitude or ELA (Carrasco et al., 2008), this latter in turn being a main parameter needed to understand glacier behaviour. The ELA in the study area is at 2800 m a.s.l in the northern volcanoes at 36°S, and smoothly descends in altitude towards southern latitudes, reaching a minimum at Volcán Hudson, where it is estimated to be at 1300 m a.s.l. In a regional context of altitudinal increase of the ELAs, with higher ice ablation and the shift to liquid precipitation, a mass imbalance must be expected on the glaciers (Carrasco et al., 2005).

Due to the approximately conical morphology of most of the ice-capped volcanoes in the study area, the hypsometric curves of the glaciers are steep at the ELA position. Therefore, a small migration to higher ground of the ELA will have a minor effect on the Accumulation Area Ratio (AAR) of these glaciers, and consequently the amount of snow fall they receive will not change significantly. This is the case of *Callaqui, Villarrica, Osorno* and *Melimoyu*, where glacier retreats can be largely explained by the interplay of these climate-related factors with micro topography and meteorology, and additionally at Villarrica, by effects of eruptions and permanent fumaroles.

At volcanoes without a conical morphology, the glaciers are located within calderas surrounded by a volcanic rim rising a few hundred meters above the main ice plateau. In these cases if the ELA is located at an altitude close to the main glacier plateau height, its migration upwards will imply a major AAR change in favour of ablation increase. This is the case of *Volcán Sollipulli*, where the ELA is within the caldera, and during the summers the whole glacier is an ablation zone. Therefore, glacier retreat observed at this present-day inactive volcano has likely been enhanced by these climate-related effects. This is unlikely at *Volcán Hudson*, as the ELA at 1300 m a.s.l. is well below the height of the caldera (1900 m a.s.l.), and therefore its altitudinal migration is not significantly affecting the AAR of this glacier nor the amount of precipitation falling as snow. Snow accumulation is very high and this allows the glacier to recover after eruptive events, i.e. 1971 and 1991.

In spite of these primary climatic influences, regional volcanism has impacted glacier fluctuations at different levels, but especially at those most active in historical times. Glacier areal reductions in the SVZ ranged from a minimum of -0.07 km^2 a^{-1} at *Mentolat*, a volcano with one of the smallest ice caps, up to a maximum of -1.16 km^2 a^{-1} at Volcán Hudson. These trends have also been accompanied by frontal retreats which are apparently enhanced during and/or after the most significant volcanic cycles since the 1970s. These volcano-related responses are supported by the fact that glacier cover on more active or younger vents showed more instability when compared to the less active units of the same volcanic complexes. Based on these statements, it is clear that volcanic activity should trigger non climatic glacier responses.

At the *Nevados de Chillán* complex, ice area losses between 1975 and 1989 may be explained largely by the eruptive cycle from 1973 to 1986 affecting the SE vents, when the result was the formation of new Volcán Arrau (Dixon et al., 1999). Only isolated ice patches remain from the former glacier in the south, however, in the northwestern sub-complex Cerro Blanco, presently less active than Volcán Viejo-Volcán Chillán, a prominent glacier reduction around its crater is denoted from the satellite images from this time. Hence, glacier reduction is very likely the consequence of ash falling during the 1973–1986 cycle characterised by frequent freatomagmatic eruptions, dacitic lava flows, ashes and pyroclast ejections (González-Ferrán, 1995). The most recent eruptive activity in 2003 must also have had the potential to impact glacier cover in a severe way as a new crater was formed between Arrau and Nuevo cones (Naranjo and Lara, 2004). This may be reflected in the increase in recent years in the number of ice bodies to the detriment of net areas. Hence, the ice reduction since 1989 has remained at a high level ($\sim$60%).

In the case of *Volcán Michinmahuida* the long term frontal retreats are well correlated with variations of other glaciers in the rest of Chile, whether in volcanic or non-volcanic mountains affected by similar climatic changes. On a shorter timescale, however, the thick ash layer from nearby Volcán Chaitén in 2008–2009 is very likely to have affected the Volcán Michinmahuida glaciers by decreasing their surface albedo. This in turn, is a plausible explanation for increased melting water produced at the surface, then percolated to the bedrock, which enhances subglacial melting and basal sliding. As a result, the rapid advance of Glaciar Amarillo and other glaciers between late 2007 and early 2009 (not enough though, to be reflected as area change in Fig. 6) may correlate with the Chaitén eruption in May 2008 which lasted until early 2009.

The plinian activity of Volcán Hudson has provoked the most dramatic effects on ice-capped volcanoes from the SVZ. Both in 1971 and 1991, part of the ice infilling the caldera was suddenly destroyed, leading to huge lahars in the valleys of Glaciar Huemules and Río Ibañez. New cones appeared at the caldera, in areas previously ice-covered, together with concentric crevasses and lagoons. One interesting finding is the transition between ice wastage and the post eruptive recovery, where a set of satellite imagery which captured the latest period of activity, has revealed a dynamic history of climate-volcano-glacier interactions characterised by high snow accumulation, generation of laharic flows and rapid ice melting events.

6. Concluding remarks

This work has provided an overview of glacier variations and ice–volcano interactions along the Southern Volcanic Zone of the Chilean Andes; a region undergoing precipitation reduction and upper atmosphere warming, triggering a general trend of glacier area shrinkage and frontal retreat. Glaciers on ice-capped volcanoes are also affected by volcanic factors which have a significant role in altering or enhancing trends depending on activity types and recurrences. The selected volcanoes have experienced a broad range of responses, from small glacier advances (Glaciar Amarillo at Volcán Michinmahuida concurrent with the 2008 eruption of nearby Volcán Chaitén) up to almost total ice disappearance (Glaciar Huemules at Volcán Hudson) after the 1971 and 1991 eruptions.

The study of these contrasting glacier responses and the identification of specific ice–volcano interactions within the region are crucial. In a volcanic country like Chile, hazards imposed by lahars and other volcanic processes have affected, and certainly can continue affecting, our population and economy. The most recent explosive events like Chaitén and Cordón Caulle are examples of the destructive power and hazardous nature of lahar flows and of the high potential of dormant but historically active volcanoes when they reactivate.

Acknowledgements

This research has been supported by FONDECYT grant #1090387 and Centro de Estudios Científicos (CECs). CECs is funded by the Chilean Government through the Centers of Excellence Base Financing Program of CONICYT. We acknowledge the GLIMS project, which has made possible the free availability of satellite images. Andrés Rivera is a Guggenheim fellow. Claudio Bravo, Sebastián Viveros and Pablo Zenteno provided data for this paper. We thank David Farías, Jonathan Oberreuter, Dennys Caro and Flavia Burger for their help in data processing and figure preparation. Ben Brock (UK) improved the English of the manuscript. Three referees gave valuable input on the content and format of the paper.

References

Aceituno, P., Fuenzalida, H., Rosenblüth, B., 1993. Climate along the extratropical west coast of South America. In: Mooney, H.A. (Ed.), Earth System Responses to Global Change: Contrasts between North and South America. Academic Press, San Diego, pp. 61–69.

Alfano, F., Bonadona, C., Volentik, A.C.M., Connor, Ch. B., Watt, S.F.L., Pyle, D.M., Connor, L.J., 2010. Tephra stratigraphy and eruptive volume of the May, 2008, Chaitén eruption, Chile. Bulletin of Volcanology 73, 613–630.

Aniya, M., Sato, H., Naruse, R., Skvarca, P., Casassa, G., 1997. Recent variations in the Southern Patagonia Icefield, South America. Arctic, Antarctic and Alpine Research 29 (1), 1–12.

Bown, F., Rivera, A., 2007. Climate changes and recent glacier behaviour in the Chilean Lake District. Global and Planetary Change 59, 79–86.

Bown, F., Rivera, A., Acuña, C., Casassa, G., 2007. Recent glacier mass balance calculations at Volcán Mocho-Choshuenco (40°S), Chilean Lake District. In: Ginot, P. (Ed.). In: Sicart, J.E. (Ed.), Glacier Mass Balance Changes and Meltwater Discharge, vol. 318. IAHS Publ, Wallingford, Oxfordshire, pp. 143–152.

Branney, M., Gilbert, J., 1995. Ice-melt collapse pits and associated features in the 1991 lahar deposits of Volcán Hudson, Chile: criteria to distinguish eruption-induced glacier melt. Bulletin of Vulcanology 57, 293–302.

Brüggen, J., 1950. Fundamentos de geología de Chile. Instituto Geográfico Militar, Santiago, 374 p.

Calder, E.S., Harris, A.J.L., Peña, P., Pilger, E., Flynn, L.P., Fuentealba, G., Moreno, H., 2004. Combined thermal and seismic analysis of the Villarrica volcano lava lake, Chile. Revista Geológica de Chile 31 (2), 259–272.

Carn, S.A., Pallister, J.S., Lara, L., Ewert, J.W., Watt, S., Prata, A.J., Thomas, R.J., Villarosa, G., 2009. The unexpected awakening of Chaitén Volcano, Chile. EOS, Transactions, American Geophysical Union 90 (24), 205–206.

Carrasco, J., Casassa, G., Quintana, J., 2005. Changes of the 0°C isotherm and the equilibrium line altitude in central Chile during the last quarter of the 20th century. Hydrological Sciences Journal 50 (6), 933–948.

Carrasco, J., Osorio, R., Casassa, G., 2008. Secular trend of the equilibrium-line altitude on the western side of the Southern Andes, derived from radiosonde and surface observations. Journal of Glaciology 54 (186), 538–550.

Cas, R., Wright, J., 1987. Volcanic Successions: Modern and Ancient. Unwin and Hyman, London, 528 p.

Castro, J.M., Dingwell, D.B., 2009. Rapid ascent of rhyolitic magma at Chaitén volcano, Chile. Letters of Nature 461, 780–784.

Castruccio, A., Clavero, J., Rivera, A., 2010. Comparative study of lahars generated by the 1961 and 1971 eruptions of Calbuco and Villarrica volcanoes, Southern Andes of Chile. Journal of Volcanology and Geothermal Research 190 (3–4), 297–311.

Cembrano, J., Lara, L., 2009. The link between volcanism and tectonics in the southern volcanic zone of the Chilean Andes: a review. Tectonophysics 471 (1–2), 96–113.

Cembrano, J., Hervé, F., Lavenu, A., 1996. The Liquiñe Ofqui fault zone: a long-lived intra-arc fault system in southern Chile. Tectonophysics 259 (1–3), 55–66.

Clavero, J., Moreno, H., 2004. Evolution of Villarrica volcano. Boletín. In: Lara, L., Clavero, J. (Eds.), Villarrica Volcano (39.5°S), Southern Andes, Chile, vol. 61. Sernageomin, Santiago, pp. 17–27.

Dixon, J., Murphy, D., Sparks, J., Chávez, R., Naranjo, J., Dunkley, P., Gilbert, J., Pringle, M., 1999. The geology of Nevados de Chillán volcano, Chile. Revista Geológica de Chile 31 (2), 161–206.

D'Orazio, M., Innocenti, F., Manetti, P., Tamponi, M., Tonarini, S., González-Ferrán, O., Lahsen, A., Omarini, R., 2003. The Quaternary calc-alkaline volcanism of the Patagonian Andes close to the Chile triple junction: geochemistry and petrogenesis of volcanic rocks from the Cay and Maca volcanoes (458S, Chile). Journal of South American Earth Sciences 16 (4), 219–242.

Falvey, M., Garreaud, R., 2009. Regional cooling in a warming world: recent temperature trends in the Southeast Pacific and along the West Coast of Subtropical South America (1979–2006). Journal of Geophysical Research 114, D04102. http://dx.doi.org/10.1029/2008JD010519.

Fournier, T., Pritchard, M., Riddick, S., 2010. Duration, magnitude, and frequency of subaerial volcano deformation events: new results from Latin America using InSAR and a global synthesis. Geochemistry, Geophysics, Geosystems 11 (1), Q01003. http://dx.doi.org/10.1029/2009GC002558.

Fuenzalida, R., 1976. The Hudson Volcano. In: González, O. (Ed.), Proceedings of the Symposium on Andean and Antarctic Volcanology Problems. Napoli, Italy, 78–87.

Fuenzalida, R., Espinosa, W., 1974. Hallazgo de una caldera volcánica en la provincia de Aisén. Revista Geológica de Chile 1, 64–66.

Giese, B., Urizar, C., Fuckar, S., 2002. Southern Hemisphere origins of the 1976 climate shift. Geophysical Research Letters 29 (2). http://dx.doi.org/10.1029/2001GL013268.

Gilbert, J., Stasiuk, M., Lane, S., Adam, C., Murphy, M., Sparks, S., Naranjo, J., 1996. Non-explosive constructional evolution of the ice-filled Caldera at Volcán Sollipulli, Chile. Bulletin of Volcanology 58, 67–83.

González-Ferrán, O., 1995. Volcanes de Chile. Instituto Geográfico Militar, Santiago, 635 p.

Gutiérrez, F., Gioncada, A., González-Ferrán, O., Lahsen, A., Mazzuoli, R., 2005. The Hudson Volcano and surrounding monogenetic centres (Chilean Patagonia): an example of volcanism associated with ridge–trench collision environment. Journal of Volcanology and Geothermal Research 145, 207–233.

Hervé, F., Faúndez, V., Calderón, M., Massone, H., Willner, A.P., 2007. Metamorphic and plutonic basement complexes. In: Moreno, T., Gibbons, W. (Eds.), The Geology of Chile. The Geological Society, London, pp. 5–19.

Hervé, F., Quiroz, D., Duhart, P., 2009. Main geological aspects of the Chilean Fjord Region. In: Häussernmann, V., Försterra, G. (Eds.), Marine Benthic Fauna of Chilean Patagonia. Nature in Focus, Santiago, pp. 30–42.

Hildreth, W., Drake, R., 1992. Volcán Quizapu, Chilean Andes. Bulletin of Volcanology 54, 93–125.

Jacob, T., Wahr, J., Pfeffer, T., Swenson, S., 2012. Recent contributions of glaciers and ice caps to sea level rise. Nature 482, 514–518.

Kääb, A., Huggel, C., Paul, F., Wessels, R., Raup, B., Kieffer, H., Kargel, J., 2003. Glacier monitoring from ASTER imagery: accuracy and application. EARSeL eProceedings 2 (1), 43–53.

Kargel, J., Abrams, M., Bishop, M., Bush, A., Hamilton, G., Jiskoot, H., Kääb, A., Kieffer, H., Lee, E., Paul, F., Rau, F., Raup, B., Shroeder, J., Soltesz, D., Stainforth, D., Stearns, L., Wessels, R., 2005. Multispectral imaging contributions to global land ice measurements from space. Remote Sensing of Environment 99, 187–2190.

Kargel, J. (Ed.), 2013. Global Land Ice Measurements from Space. Praxis-Springer, Heidelberg, ISBN 978-3-540-79817-0.

Kratzmann, D.J., Carey, S., Scasso, R., Naranjo, J.A., 2009. Compositional variations and magma mixing in the 1991 eruptions of Hudson volcano, Chile. Bulletin of Volcanology 71, 419–439.

Lange, D., Cembrano, J., Rietbrock, A., Haberland, C., Dahm, T., Bataille, K., 2008. First seismic record for intra-arc strike-slip tectonics along the Liquiñe-Ofqui fault zone at the obliquely convergent plate margin of the Southern Andes. Tectonophysics 455 (1–4), 14–24.

Lara, L., 2004. Overview of Villarrica Volcano. Boletín. In: Lara, L., Clavero, J. (Eds.), Villarrica Volcano (39.5°S), Southern Andes, Chile, vol. 61. Sernageomin, Santiago, pp. 5–12.

Lara, L., Cembrano, J., Lavenu, A., 2008. Quaternary vertical displacement along the Liquiñe-Ofqui fault zone: differential uplift and coeval volcanism in the Southern Andes? International Geology Review 50, 1–19.

Legrand, M., Wagenbach, D., 1999. Impact of the Cerro Hudson and Pinatubo volcanic eruptions on the Antarctic air and snow chemistry. Journal of Geophysical Research 104 (D1), 1581–1596.
Leprince, S., Barbot, S., Ayoub, F., Avouac, J., 2007. Automatic and precise orthorectification, coregistration, and subpixel correlation of satellite images, application to ground deformation measurements. IEEE Transactions on Geoscience and Remote Sensing 45 (6), 1529–1558.
López-Escobar, L., Cembrano, J., Moreno, H., 1995. Geochemistry and tectonics of the Chilean Southern Andes basaltic Quaternary volcanism (37°–46°S). Revista Geológica de Chile 22 (2), 219–234.
Major, J.J., Newhall, C.G., 1989. Snow and ice perturbation during historical volcanic eruptions and the formation of lahars and floods. A global review. Bulletin of Volcanology 52, 1–27.
Masiokas, M., Rivera, A., Espizúa, L., Villalba, R., Delgado, S., Aravena, J.C., 2009. Glacier fluctuations in extratropical South America during the past 1000 years. Palaeogeography, Palaeoclimatology, Palaeoecology 281, 242–268.
Mee, K., Tuffen, H., Gilbert, J., 2006. Snow-contact volcanic facies at Nevados de Chillan volcano, Chile, and implications for reconstructing past eruptive environments. Bulletin of Volcanology 68, 363–376.
Mee, K., Gilbert, J.S., McGarvie, D.W., Naranjo, J.A., Pringle, M.S., 2009. Palaeoenvironment reconstruction, volcanic evolution and geochronology of the Cerro Blanco subcomplex, Nevados de Chillán volcanic complex, central Chile. Bulletin of Volcanology 71 (8), 933–952.
Montecinos, A., Aceituno, P., 2003. Seasonality of the ENSO-related rainfall variability in Central Chile and associated Circulation Anomalies. Journal of Climate 16 (2), 281–296.
Moreno, H., 2000. Mapa de Peligros Volcánicos del volcán Villarrica. Documentos de trabajo #17. Servicio Nacional de Geología y Minería. scale 1:75.000.
Naranjo, J., Stern, C., 1998. Holocene explosive activity of Hudson volcano, Southern Andes. Bulletin of Volcanology 59, 291–306.
Naranjo, J.A., Lara, L., 2004. August-September 2003 small vulcanian eruption at the Nevados de Chillán Volcanic Complex (36°50'S), Southern Andes (Chile). Revista Geológica de Chile 31 (2), 359–366.
Naranjo, J.A., Moreno, H., 2004. Laharic debris-flows from Villarrica Volcano. Boletín. In: Lara, L., Clavero, J. (Eds.), Villarrica Volcano (39.5°S), Southern Andes, Chile, vol. 61. Sernageomin, Santiago, pp. 28–45.
Naranjo, J.A., Stern, C., 2004. Holocene tephrochronology of the southernmost part (42°30′–45°S) of the Andean Southern Volcanic Zone. Revista Geológica de Chile 31 (2), 225–240.
Naranjo, J.A., Gilbert, J.S., Sparks, R.S.J., 2008. Geología del Complejo Volcánico Nevados de Chillán, Región del Biobío. No.114, 28 p., 1 mapa escala 1:50.000. In: Carta Geológica de Chile, Serie Geología Básica. Servicio Nacional de Geología y Minería, Santiago. ISSN 0717-7283.
Newhall, C., Punongbayan, R., 1996. Fire and Mud, Eruptions and Lahars of Mount Pinatubo, Philippines. University of Washington Press, Seattle, 1126 p.
Orihashi, Y., Naranjo, J., Motoki, A., Sumino, H., Hirata, D., Anma, R., Nagao, K., 2004. Quaternary volcanic activity of Hudson and Lautaro Volcanoes, Chilean Patagonia: new constraints from K–Ar ages. Revista Geológica de Chile 31, 207–224.
Pankhurst, R.J., Hervé, F., Rojas, L., Cembrano, J., 1992. Magmatism and tectonics in continental Chiloé, Chile (42°–42°30′S). Tectonophysics 205 (1–3), 283–294.
Petit-Breuilh, M., 1995. Volcanic History of Nevados de Chillán Volcano, Chile. British Geological Survey. Technical Report. WC/95/82.
Petit-Breuihl, M., Lobato, J., 1994. Cronología eruptiva histórica del volcán Villarrica, Andes del Sur. Abstracts of the VIIth Chilean Geological Congress, Concepción.Philippi, R. 1862. Viaje a los Baños y al nuevo Volcán de Chillán. Anales de la Universidad de Chile 20, 279–309.
Philippi, R., 1862. Viaje a los Baños y al nuevo Volcán de Chillán. Anales de la Universidad de Chile 20, 279–309.
Pritchard, M.E., Simons, M., 2004. An InSAR-based survey of volcanic deformation in the Southern Andes. Geophysical Research Letters 31, L15610. http://dx.doi.org/10.1029/2004GL020545.
Quintana, J., Aceituno, P., 2012. Changes in the rainfall regime along the extratropical west coast of South America (Chile): 30–43° S. Atmósfera 25 (1), 1–22.
Radic, J.P., 2010. Las cuencas cenozoicas y su control en el volcanismo de los Complejos Nevados de Chillan y Copahue-Callaqui (Andes del Sur, 36–39°S). Andean Geology 37 (1), 220–246.
Rignot, E., Rivera, A., Casassa, G., 2003. Contribution of the Patagonia Icefields of South America to Sea Level Rise. Science 302, 434–436.
Rivera, A., 1989. Inventario de glaciares entre las cuencas de los ríos Bio Bio y Petrohué. Su relación con el volcanismo activo: Caso del volcán Lonquimay. Informe de practica profesional, Universidad de Chile. Undergraduate thesis, University of Chile.
Rivera, A., Acuña, C., Casassa, G., Bown, F., 2002. Use of remote sensing and field data to estimate the contribution of Chilean glaciers to the sea level rise. Annals of Glaciology 34, 367–372.
Rivera, A., Bown, F., Casassa, G., Acuña, C., Clavero, J., 2005. Glacier shrinkage and negative mass balance in the Chilean Lake District (40°S). Hydrological Sciences Journal 50 (6), 963–974.
Rivera, A., Bown, F., Mella, R., Wendt, J., Casassa, G., Acuña, C., Rignot, E., Clavero, J., 2006. Ice volumetric changes on active volcanoes in Southern Chile. Annals of Glaciology 43, 111–122.
Rivera, A., Benham, T., Casassa, G., Bamber, J., Dowdeswell, J., 2007. Ice elevation and areal changes of glaciers from the Northern Patagonia Icefield, Chile. Global and Planetary Change 59, 126–137.
Rivera, A., Bown, F., Acuña, C., Ordenes, F., 2008a. Chilean glaciers as indicators of climate change. Terra Glacialis 11, 193–207.
Rivera, A., Corripio, J.G., Brock, B., Clavero, J., Wendt, J., 2008b. Monitoring ice capped active volcán Villarrica in southern Chile by means of terrestrial photography combined with automatic weather stations and GPS. Journal of Glaciology 54 (188), 920–933.
Rivera, A., Bown, F., Carrión, D., Zenteno, P., 2012. Glacier responses to recent volcanic activity in Southern Chile. Environmental Research Letters 7, 014036. http://dx.doi.org/10.1088/1748-9326/7/1/014036.
Rodríguez, C., Pérez, Y., Moreno, H., Clayton, J., Antinao, J., Duhart, P., Martin, M., 1999. Geologic Map of the Panguipulli-Riñihue Area, Lake Region, 1:100 000 Scale. Geologic Maps Series no. 10. Chilean Geological Survey.
Romero, J.E., 2012. Some backgrounds on the short October 2011 eruption at Mt. Hudson, 45°30′S, Southern Andes. Pyroclastic flow. Journal of Geology 1 (1), 1–8.
Rosenblüth, B., Fuenzalida, H., Aceituno, P., 1997. Recent temperature variations in Southern South America. International Journal of Climatology 17, 67–85.
Simkin, T., Siebert, L., 2000. Earth's volcanoes and eruptions: an overview. In: Sigurdsson, H. (Ed.), Encyclopedia of Volcanoes. Academic Press, San Diego, pp. 249–261.
Simkin, T., Siebert, L., 2002. Global Volcanism FAQs. Smithsonian Institution. Global Volcanism Program Digital Information Series, GVP-5. http://www.volcano.si.edu/education/questions/.
Singer, B.S., Jicha, B.R., Harper, M.A., Naranjo, J.A., Lara, L.E., Moreno, H., 2008. Eruptive history, geochronology, and magmatic evolution of the Puyehue-Cordón Caulle volcanic complex, Chile. GSA Bulletin 120 (5–6), 599–618.
Stern, C., 1991. Mid-Holocene tephra on Tierra del Fuego (54°S) derived from the Hudson volcano (46°S): evidence for a large explosive eruption. Revista Geológica de Chile 18, 139–146.
Stern, C., 2004. Active Andean volcanism: its geologic and tectonic setting. Revista Geológica de Chile 31 (2), 161–206.
Thouret, J., Ramirez, J., Gilbert-Malengreau, B., Vargas, C.A., Naranjo, J.L., Vandemeulebrouck, J., Valla, F., Funk, M., 2007. Volcano-glacier interactions on composite cones and lahar generation: the Nevado (Colombia) case study. Annals of Glaciology 45, 115–127.
Trabant, D.C., Waitt, R.B., Major, J.J., 1994. Disruption of Drift glacier and origin of floods during the 1989–1990 eruptions of Redoubt Volcano, Alaska. Journal of Volcanology and Geothermal Research 62, 369–385.
Voight, B., 1996. The management of Volcano Emergencies: Nevado del Ruiz. In: Scarpa, R., Tilling, R. (Eds.), Monitoring and Mitigation of Volcano Hazards. Springer, Berlin, pp. 719–770.
Warren, C., Aniya, M., 1999. The calving glaciers of Southern South America. Global and Planetary Change 22, 59–77.
Watt, S., Pyle, M., Mather, T., Martin, R., Matthews, N., 2009. Fallout and distribution of volcanic ash over Argentina following the May 2008 explosive eruption of Chaitén, Chile. Journal of Geophysical Research 114, B04207. http://dx.doi.org/10.1029/2008JB006219.
Wilson, T.M., Cole, J.W., Stewart, C., Cronin, S.J., Johnston, D.M., 2011. Ash storms: impacts of wind-remobilised volcanic ash on rural communities and agriculture following the 1991 Hudson eruption, southern Patagonia, Chile. Bulletin of Volcanology 73, 223–239.
Witter, J.B., Delmelle, P., 2004. Acid gas hazards in the crater of Villarrica volcano (Chile). Revista Geológica de Chile 31 (2), 273–277.
Witter, J., Kress, V., Delmelle, P., Stix, J., Fuentealba, G., 2004. Volatile degassing, petrology, and magma dynamics of the Villarrica lava lake, southern Chile. Journal of Volcanology and Geothermal Research 134 (4), 303–337.
Zellmer, G. F., Freymuth, H., Cembrano, J. M., Clavero, J. E., Veloso, E. A. E., Siefeld, G. G. Altered mineral uptake into fresh arc magmas: insights from U-Th isotopes of samples from Andean volcanoes under differential crustal stress regimes. GSL Special Volume on Orogenic Andesites and Crustal Growth, in press.